Astronomy Letters, Vol. 20, No. 5, 1994, pp. 651 - 657. Translated from Pis'ma v Astronomicheskii Zhurnal, Vol. 20, No. 10, 1994, pp. 754 - 761.

Singular Mixing in Stars

N. A. Inogamov

Institute of Theoretical Physics, Russian Academy of Sciences, Vorob'evskoe sh., Moscow, 117940 Russia

Received June 17, 1994

Abstract – Departures from equilibrium and the associated symmetry breakdown are known to play an important role in astrophysics. They lead to spatial anisotropy, as well as to anisotropy of thermodynamic properties, to mixing of stratified layers, to changes of average properties, etc. Examples of such departures are fragmentation and the formation of fibrils and filaments. Such departures may be due either to instability of stratified layers in a gravitational field (Rayleigh–Taylor instability) or to velocity-field fluctuations (Richtmyer–Meshkov instability). The simplest stratification model is obtained in a two-zone approximation with a density jump at the contact boundary. This dynamical system was investigated. It is shown that the evolution of such contact boundaries is not smooth. In particular, over a finite time interval, singularity appears at the contact boundary, which leads to nondifferentiability of the functions and discontinuous jumps at the boundary, where initially all the functions were infinitely differentiable. Such an evolution is not restricted by a special family of solutions. On the contrary, singularity appears under arbitrary initial conditions. These phenomena result in both an increase in the mixing rate and a decrease in the mixing zone depth. They may also be responsible for the sharper profiles of flares, ejecta, etc.

The problem of the destruction of contact boundaries that separate media with different densities and temperatures is of great importance for various applications. This problem is closely connected with the theory of turbulent surface mixing, as well as with hydrodynamic Rayleigh–Taylor, Richtmyer–Meshkov, and Kelvin–Helmholtz instabilities accompanying the explosions of supernovae [1 - 8], fragmentation in planetary nebulae [9, 10] and Wolf–Rayet stars [11], accretion onto compact magnetized objects [12, 13], etc. Similar problems arise in studies of subsonic stellar convection (for example, solar granulation [14]), where the Boussinesq approximation is not valid.

Consider the evolution of instability. The initial perturbation will be periodic along the surface. As a rule, the evolution of the free surface S_f is assumed to be monotonic (see Fig. 1, where the symmetric half of the period is displayed). For an initially slightly corrugated surface, the singularities are most distant from the surface. The singularities are assumed to asymptotically approach the surface. The wind from the singularities pushes away the Lagrangian particles. This process leads to the formation of dents ("bubbles") on the free surface, with the top of a bubble being the retardation point of two opposite flows.

In this paper, it is shown that the evolution (in particular, the freezing of singularities) proceeds in a way different than that described above. The nearest singularity does not freeze at a finite distance from S_f and coincides with the surface. Below, we evaluate the time of coincidence t_c, as well as the bubble amplitude $\eta_{0,c}$ at the instant of coincidence.

The surface S_f and the fluid enclosed by this surface obey the well-known classic equations with the relevant boundary conditions

$$\Delta\varphi = 0, \quad \varphi_t|_\eta = -v^2/2|_\eta - p|_\eta - g\eta, \quad \eta_t = \varphi_y|_\eta - \varphi_x|_\eta \eta_x. \tag{1}$$

The perturbation of the flat surface is considered, where the x and y axes of the laboratory frame are directed along the surface and inwardly, respectively. The analysis is limited by the assumption that the density of one of the fluids may be disregarded. Assume that $\rho = 1$ and that the acceleration is $g = 0, \pm 1$. The case $g = 0$ corresponds to the Richtmyer–Meshkov instability with initial linear perturbations when the speed of the entropy turbulent modes is small in comparison with the velocity of a shock wave (and, therefore, with the sound speed behind the shock front). This fact implies that compressibility can be disregarded. The cases $g = 1$ and $g = -1$ correspond to the Rayleigh–Taylor instability and gravity waves, respectively. The following units are used: $|g| = k = 1$ for $g = \pm 1$ and $|w_0| = k = 1$ for the Richtmyer–Meshkov instability, where w_0 is the initial velocity at $x = 0$. In equations (1), assume that $\mathbf{v} = \nabla\varphi$. Hereafter, subscripts designate differentiation with respect to the corresponding variable. The boundary is given by the function $y = \eta(x, t)$.

Consider the expansion in harmonics of the periodical perturbation:

$$\varphi = \sum \tilde{a}_n c_n e_n / n, \quad c_n = \cos(nx), \quad e_n = \exp(-ny). \tag{2}$$

1063-7737/94/2005-0651$10.00 © 1994 МАИК Наука/Interperiodica Publishing

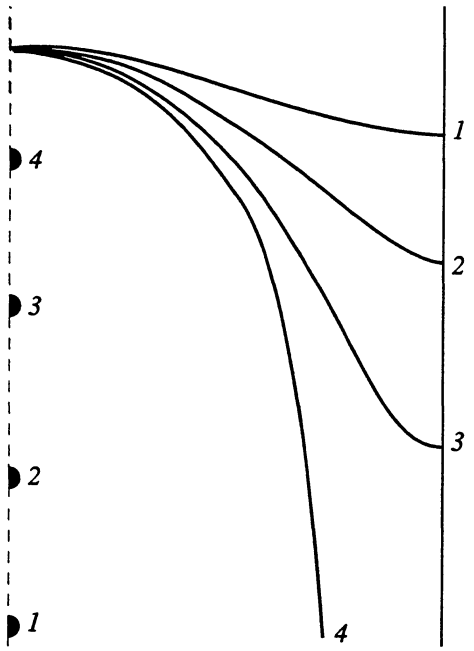

Fig. 1. Typical illustration of the monotonic evolution of the boundary and the approaching of potential singularities (semicircles show the instantaneous location of the nearest singularity). Motion is represented in acomoving frame of the top of the bubble. The numbers *1*, *2*, *3*, and *4* correspond to instants of time. Number *4* corresponds to the asymptotic state when the nearest singularity is frozen at a distance of ~1.2/k from the top.

Amplitudes $\tilde{a}_n(t)$ are real functions. Then, for $g = -1$, expansion (2) leads to standing waves. Below, this consideration is limited by Rayleigh–Taylor and Richtmyer–Meshkov instabilities. For periodical perturbations, the surface S_f is obviously characterized by alternating convex and concave areas. These areas are defined as bubbles and streams, respectively. The top of a bubble is at $x = 0$. The power series expansion of η over higher orders of curvature is

$$\eta = \sum \eta_j x^{2j} = \eta_0(t) + \eta_1(t)x^2 + \eta_2(t)x^4 + \ldots \quad (3)$$

Initially, the kinematic boundary condition is considered. Expansions are substituted for φ and η, and cosine and exp are expanded into power series. Then, the right-hand side of the boundary condition is

$$\sum_{s=0}\sum_{p=0}\frac{(-1)^{p+s}}{(2p)!s!}\left[-m_{2p+s} + \frac{2\left(\sum j\eta_j x^{2j}\right)m_{2p+s+1}}{2p+1}\right]x^{2p}\left(\sum_{j=1}\eta_j x^{2j}\right)^s, \quad (4)$$

$$m_j = \sum n^j a_n, \quad n = 1, 2, \ldots \quad (5)$$

The amplitudes a_n on the right-hand side of expression (5) for the moments m_j that appear on the right-hand side of (4) are given in a comoving frame with the origin at the top of the bubble. These amplitudes are related to those measured in the laboratory frame by $a_n = \tilde{a}_n \exp(-n\eta_0)$. Then, the right- and left-hand sides of the kinematic boundary condition are expanded into series of powers of x^2, and the coefficients are equated with the corresponding powers. After tedious algebraic manipulation, the first sixth-order differential equations for advection of the boundary with the given velocity field are obtained:

$$\dot{\eta}_1 = m_2/2 + 3m_1\eta_1,$$

$$\dot{\eta}_2 = -m_4/24 + 5(-m_3\eta_1/6 - m_2\eta_1^2/2 + m_1\eta_2),$$

$$\dot{\eta}_3 = m_6/720 + 7(m_5\eta_1/120 + m_4\eta_1^2/12 + m_3\eta_1^3/6 - m_3\eta_2/6 - m_2\eta_1\eta_2 + m_1\eta_3),$$

$$\dot{\eta}_4 = -m_8/40320 - m_7\eta_1/560 - 3m_6\eta_1^2/80 - m_5\eta_1^3/4 - 3m_4\eta_1^4/8 + 3m_5\eta_2/40 + 3m_4\eta_1\eta_2/2 + 9m_3\eta_1^2\eta_2/2 - 9m_2\eta_2^2/2 - 3m_3\eta_3/2 - 9m_2\eta_1\eta_3 + 9m_1\eta_4, \quad (6)$$

$$\dot{\eta}_5 = m_{10}/3628800 + 11(m_9\eta_1/362880 + m_8\eta_1^2/10080 + m_7\eta_1^3/720 + m_6\eta_1^4/144 + m_5\eta_1^5/120 - m_7\eta_2/5040 - m_6\eta_1\eta_2/120 - m_5\eta_1^2\eta_2/12 - m_4\eta_1^3\eta_2/6 + m_4\eta_2^2/12 + m_3\eta_1\eta_2^2/2 + m_5\eta_3/120 + m_4\eta_1\eta_3/6 + m_3\eta_1^2\eta_3/2 - m_2\eta_2\eta_3 - m_3\eta_4/6 - m_2\eta_1\eta_4 + m_1\eta_5).$$

Here the cumbersome sixth-order expression is omitted. Equations (6) are linear with respect to moments (and, therefore, with respect to amplitudes), so that they may be represented in the form $d\boldsymbol{\eta}/dt = \hat{\eta}\mathbf{m}$, where the vectors $d\boldsymbol{\eta}/dt$ and $\mathbf{m}$ consist of N and $2N$ components, respectively, and where $\hat{\eta}$ is the $N \times 2N$ rectangular matrix, the elements of which depend only on $\boldsymbol{\eta}$.

The equation of the zeroth order with respect to x^2 is $\dot{\eta}_0 = -\sum a_n$. As is shown below from the dynamical equations, the unknown variable $\eta_0(t)$ splits off from the system of equations; therefore, that equation can be integrated separately for this variable.

Now consider the dynamical equations. Initially, the acceleration potential $\varphi_t(x, y, t)$ is estimated in the laboratory frame. We have $(\partial\varphi(x, y, t)/\partial t)|_{x,y} = \sum(d\tilde{a}_n/dt)c_n e_n/n = \sum(\dot{\tilde{a}}_n e_n^0)c_n e_n^\Delta/n$, where $e_n^0 = \exp(-n\eta_0)$, $e_n^\Delta = \exp(-n\Delta)$, and $\Delta = y - \eta_0$. Estimate the acceleration at the boundary: $\varphi_t|_\eta$. We have $\Delta|_\eta =$

$\eta - \eta_0$. Expand c_n and e_n^{Δ} in series of x and Δ, respectively. The amplitudes are replaced by moments according to formulas (5). Using the relationship between $\tilde{a}_n$ and a_n, we obtain

$$\dot{\tilde{a}}_n e_n^0 = \dot{a}_n + n\dot{\eta}_0 a_n, \quad \sum_n n^j \dot{\tilde{a}}_n e_n^0 = \dot{m}_j + \dot{\eta}_0 m_{j+1},$$

$$\dot{m}_j = \sum n^j \dot{a}_n.$$

Finally, we obtain

$$\varphi_t(x, y, t)|_{y=\eta} = \sum_{s=0}\sum_{p=0} (-1)^{p+s}/((2p)!s!) \times (\dot{m}_{2p+s-1} + \dot{\eta}_0 m_{2p+s}) x^{2p} (\Delta|_\eta)^s. \quad (7)$$

Now estimate the density of kinetic energy. From (2), $v^2 = \varphi_x^2 + \varphi_y^2 = \sum\sum \tilde{a}_n \tilde{a}_j c_{n-j} e_{n+j}$. Expanding v^2 in power series of x^2 and $(y - \eta_0)$, respectively, we have

$$v^2 = \sum_s\sum_p\sum_n\sum_j (-1)^{p+s}/((2p)!s!) \times (n-j)^{2p} (n+j)^s a_n a_j x^{2p} (y-\eta_0)^s.$$

Expanding $(n-j)^{2p}$ and $(n+j)^s$ according to the binomial theorem and using (5), we have

$$v^2(x, y, t) = \sum_{s=0}\sum_{p=0}\sum_{a=0}^{2p}\sum_{b=0}^{s} \frac{(-1)^{p+s+a}}{a!b!(2p-a)!(s-b)!} \times m_{a+b} m_{2p+s-a-b} x^{2p} (y-\eta_0)^s. \quad (8)$$

Now expressions (7) and (8) are substituted into the right- and left-hand sides of the dynamical boundary condition (1), respectively. The quantity $\dot{\eta}_0$ is replaced by the amplitudes, in accordance with the equation $\dot{\eta}_0 = -m_0$. The left- and right-hand sides are expanded in power series of x^2, and the corresponding coefficients are equated. The zeroth-order equation involving η_0 should be omitted because of calibration considerations, because the dynamical boundary condition is correct to an arbitrary function of time. In the following six orders, we obtain

$$\text{lhs}_1 = -\dot{m}_1/2 - \dot{m}_0\eta_1,$$

$$\text{lhs}_2 = \dot{m}_3/24 + \dot{m}_2\eta_1/2 + \dot{m}_1\eta_1^2/2 - \dot{m}_0\eta_2,$$

$$\text{lhs}_3 = -\dot{m}_5/720 - \dot{m}_4\eta_1/24 - \dot{m}_3\eta_1^2/4 - \dot{m}_2\eta_1^3/6 + \dot{m}_2\eta_2/2 + \dot{m}_1\eta_1\eta_2 - \dot{m}_0\eta_3, \quad (9)$$

$$\text{lhs}_4 = \dot{m}_7/40320 + \dot{m}_6\eta_1/720 + \dot{m}_5\eta_1^2/48 + \dot{m}_4\eta_1^3/12 + \dot{m}_3\eta_1^4/24 - \dot{m}_4\eta_2/24 - \dot{m}_3\eta_1\eta_2/2 - \dot{m}_2\eta_1^2\eta_2/2 + \dot{m}_1\eta_2^2/2 + \dot{m}_2\eta_3/2 + \dot{m}_1\eta_1\eta_3 - \dot{m}_0\eta_4,$$

$$\text{lhs}_5 = -\dot{m}_9/3628800 - \dot{m}_8\eta_1/40320 - \dot{m}_7\eta_1^2/1440 - \dot{m}_6\eta_1^3/144 - \dot{m}_5\eta_1^4/48 - \dot{m}_4\eta_1^5/120 + \dot{m}_6\eta_2/720 + \dot{m}_5\eta_1\eta_2/24 + \dot{m}_4\eta_1^2\eta_2/4 + \dot{m}_3\eta_1^3\eta_2/6 - \dot{m}_3\eta_2^2/4 - \dot{m}_2\eta_1\eta_2^2/2 - \dot{m}_4\eta_3/24 - \dot{m}_3\eta_1\eta_3/2 - \dot{m}_2\eta_1^2\eta_3/2 + \dot{m}_1\eta_2\eta_3 + \dot{m}_2\eta_4/2 + \dot{m}_1\eta_1\eta_4 - \dot{m}_0\eta_5,$$

$$\text{rhs}_1 = -m_1^2/2 - g\eta_1,$$

$$\text{rhs}_2 = -m_2^2/8 + m_1m_3/6 + m_1m_2\eta_1/2 - m_1^2\eta_1^2/2 - g\eta_2,$$

$$\text{rhs}_3 = -m_3^2/72 + m_2m_4/48 - m_1m_5/120 + m_2m_3\eta_1/12 - m_1m_4\eta_1/8 - m_2^2\eta_1^2/4 + m_1m_2\eta_1^3/2 + m_1m_2\eta_1\eta_2/2 - m_1^2\eta_1\eta_2 - g\eta_3,$$

$$\text{rhs}_4 = -m_4^2/1152 + m_3m_5/720 - m_2m_6/1440 + m_1m_7/5040 + m_3m_4\eta_1/144 - m_2m_5\eta_1/80 + m_1m_6\eta_1/144 - m_3^2\eta_1^2/24 + m_2m_4\eta_1^2/48 + m_1m_5\eta_1^2/24 + m_2m_3\eta_1^3/6 - m_1m_4\eta_1^3/12 - m_2^2\eta_1^4/8 - m_1m_3\eta_1^4/6 + m_2m_3\eta_2/12 - m_1m_4\eta_2/8 - m_2^2\eta_1\eta_2/2 + 3m_1m_2\eta_1^2\eta_2/2 - m_1^2\eta_2^2/2 + m_1m_2\eta_3/2 - m_1^2\eta_1\eta_3 - g\eta_4, \quad (10)$$

$$\text{rhs}_5 = -m_5^2/28800 + m_4m_6/17280 - m_3m_7/30240 + m_2m_8/80640 - m_1m_9/362880 + m_4m_5\eta_1/2880 - m_3m_6\eta_1/1440 + m_2m_7\eta_1/2016 - m_1m_8\eta_1/5760 - m_4^2\eta_1^2/288 + m_3m_5\eta_1^2/360 + m_2m_6\eta_1^2/360 - m_1m_7\eta_1^2/360 + m_3m_4\eta_1^3/48 - m_2m_5\eta_1^3/48 - m_1m_6\eta_1^3/144 - m_3^2\eta_1^4/24 - m_2m_4\eta_1^4/48 + m_1m_5\eta_1^4/24 + m_2m_3\eta_1^5/12 + m_1m_4\eta_1^5/24 + m_3m_4\eta_2/144 - m_2m_5\eta_2/80 + m_1m_6\eta_2/144 - m_3^2\eta_1\eta_2/12 + m_2m_4\eta_1\eta_2/24 + m_1m_5\eta_1\eta_2/12 + m_2m_3\eta_1^2\eta_2/2 - m_1m_4\eta_1^2\eta_2/4 - m_2^2\eta_1^3\eta_2/2 - 2m_1m_3\eta_1^3\eta_2/3 - m_2^2\eta_2^2/4 + 3m_1m_2\eta_1\eta_2^2/2 + m_2m_3\eta_3/12 - m_1m_4\eta_3/8 - m_2^2\eta_1\eta_3/2 + 3m_1m_2\eta_1^2\eta_3/2 - m_1^2\eta_2\eta_3 + m_1m_2\eta_4/2 - m_1^2\eta_1\eta_4 - g\eta_5.$$

For the sake of convenience, the sixth-order expressions are not given. The left-hand (lhs) and right-hand

sides (rhs) of the dynamical equations are given by formulas (9) and (10), respectively. The terms in $(\mathrm{rhs})_i$ quadratic in m_j [and, as follows from (5), quadratic in a_j] give the expansion coefficients for v^2 at the boundary. The last term of $(\mathrm{rhs})_i$, equal to $(-g\eta_i)$, is due to the gravitational potential. Derivatives $\dot{m}_j$ with $j = 0, 1, \ldots, (2i-1)$ involve $(\mathrm{lhs})_i$. Differentiate (5) with respect to t, express $\dot{m}_j$ in terms of $\dot{a}_i$, and substitute the expressions obtained into (9). Taking into account the linearity of (lhs) with respect to $\dot{m}_j$ and $\dot{a}_i$, the following system of equations is obtained:

$$(\hat{\Gamma}\dot{\mathbf{a}})_i = (\mathrm{rhs})_i, \quad \dot{\boldsymbol{\eta}} = \hat{\eta}\mathbf{m}, \qquad (11)$$

where $\hat{\Gamma} = \hat{\Gamma}(\boldsymbol{\eta})$ is the $N \times N$ matrix, the elements of which are algebraic polynomials of η_i:

$$\Gamma_{11} = -1/2 - \eta_1, \quad \Gamma_{21} = 1/24 + \eta_1/2 + \eta_1^2/2 - \eta_2,$$

$$\Gamma_{12} = -1 - \eta_1, \quad \Gamma_{22} = 1/3 + 2\eta_1 + \eta_1^2 - \eta_2,$$

$$\Gamma_{13} = -3/2 - \eta_1,$$

$$\Gamma_{23} = 9/8 + 9\eta_1/2 + 3\eta_1^2/2 - \eta_2,$$

$$\Gamma_{14} = -2 - \eta_1, \quad \Gamma_{24} = 8/3 + 8\eta_1 + 2\eta_1^2 - \eta_2,$$

$$\Gamma_{15} = -5/2 - \eta_1,$$

$$\Gamma_{25} = 125/24 + 25\eta_1/2 + 5\eta_1^2/2 - \eta_2,$$

$$\Gamma_{31} = -1/720 - \eta_1/24 - \eta_1^2/4 - \eta_1^3/6 + \eta_2/2 + \eta_1\eta_2 - \eta_3,$$

$$\Gamma_{32} = -2/45 - 2\eta_1/3 - 2\eta_1^2 - 2\eta_1^3/3 + 2\eta_2 + 2\eta_1\eta_2 - \eta_3,$$

$$\Gamma_{33} = -27/80 - 27\eta_1/8 - 27\eta_1^2/4 - 3\eta_1^3/2 + 9\eta_2/2 + 3\eta_1\eta_2 - \eta_3,$$

$$\Gamma_{34} = -64/45 - 32\eta_1/3 - 16\eta_1^2 - 8\eta_1^3/3 + 8\eta_2 + 4\eta_1\eta_2 - \eta_3,$$

$$\Gamma_{35} = -625/144 - 625\eta_1/24 - 125\eta_1^2/4 - 25\eta_1^3/6 + 25\eta_2/2 + 5\eta_1\eta_2 - \eta_3,$$

$$\Gamma_{41} = 1/40320 + \eta_1/720 + \eta_1^2/48 + \eta_1^3/12 + \eta_1^4/24 - \eta_2/24 - \eta_1\eta_2/2 - \eta_1^2\eta_2/2 + \eta_2^2/2 + \eta_3/2 + \eta_1\eta_3 - \eta_4,$$

$$\Gamma_{42} = 1/315 + 4\eta_1/45 + 2\eta_1^2/3 + 4\eta_1^3/3 + \eta_1^4/3 - 2\eta_2/3 - 4\eta_1\eta_2 - 2\eta_1^2\eta_2 + \eta_2^2 + 2\eta_3 + 2\eta_1\eta_3 - \eta_4,$$

$$\Gamma_{43} = 243/4480 + 81\eta_1/80 + 81\eta_1^2/16 + 27\eta_1^3/4 + 9\eta_1^4/8 - 27\eta_2/8 - 27\eta_1\eta_2/2 - 9\eta_1^2\eta_2/2 + 3\eta_2^2/2 + 9\eta_3/2 + 3\eta_1\eta_3 - \eta_4,$$

$$\Gamma_{44} = 128/315 + 256\eta_1/45 + 64\eta_1^2/3 + 64\eta_1^3/3 + 8\eta_1^4/3 - 32\eta_2/3 - 32\eta_1\eta_2 - 8\eta_1^2\eta_2 + 2\eta_2^2 + 8\eta_3 + 4\eta_1\eta_3 - \eta_4,$$

$$\Gamma_{45} = 15625/8064 + 3125\eta_1/144 + 3125\eta_1^2/48 + 625\eta_1^3/12 + 125\eta_1^4/24 - 625\eta_2/24 - 125\eta_1\eta_2/2 - 25\eta_1^2\eta_2/2 + 5\eta_2^2/2 + 25\eta_3/2 + 5\eta_1\eta_3 - \eta_4,$$

$$\Gamma_{51} = -1/3628800 - \eta_1/40320 - \eta_1^2/1440 - \eta_1^3/144 - \eta_1^4/48 - \eta_1^5/120 + \eta_2/720 + \eta_1\eta_2/24 + \eta_1^2\eta_2/4 + \eta_1^3\eta_2/6 - \eta_2^2/4 - \eta_1\eta_2^2/2 - \eta_3/24 - \eta_1\eta_3/2 - \eta_1^2\eta_3/2 + \eta_2\eta_3 + \eta_4/2 + \eta_1\eta_4 - \eta_5,$$

$$\Gamma_{52} = -2/14175 - 2\eta_1/315 - 4\eta_1^2/45 - 4\eta_1^3/9 - 2\eta_1^4/3 - 2\eta_1^5/15 + 4\eta_2/45 + 4\eta_1\eta_2/3 + 4\eta_1^2\eta_2 + 4\eta_1^3\eta_2/3 - 2\eta_2^2 - 2\eta_1\eta_2^2 - 2\eta_3/3 - 4\eta_1\eta_3 - 2\eta_1^2\eta_3 + 2\eta_2\eta_3 + 2\eta_4 + 2\eta_1\eta_4 - \eta_5,$$

$$\Gamma_{53} = -243/44800 - 729\eta_1/4480 - 243\eta_1^2/160 - 81\eta_1^3/16 - 81\eta_1^4/16 - 27\eta_1^5/40 + 81\eta_2/80 + 81\eta_1\eta_2/8 + 81\eta_1^2\eta_2/4 + 9\eta_1^3\eta_2/2 - 27\eta_2^2/4 - 9\eta_1\eta_2^2/2 - 27\eta_3/8 - 27\eta_1\eta_3/2 - 9\eta_1^2\eta_3/2 + 3\eta_2\eta_3 + 9\eta_4/2 + 3\eta_1\eta_4 - \eta_5,$$

$$\Gamma_{54} = -1024/14175 - 512\eta_1/315 - 512\eta_1^2/45 - 256\eta_1^3/9 - 64\eta_1^4/3 - 32\eta_1^5/15 + 256\eta_2/45 + 128\eta_1\eta_2/3 + 64\eta_1^2\eta_2 + 32\eta_1^3\eta_2/3 - 16\eta_2^2 - 8\eta_1\eta_2^2 - 32\eta_3/3 - 32\eta_1\eta_3 - 8\eta_1^2\eta_3 + 4\eta_2\eta_3 + 8\eta_4 + 4\eta_1\eta_4 - \eta_5,$$

$$\Gamma_{55} = -78125/145152 - 78125\eta_1/8064 - 15625\eta_1^2/288 - 15625\eta_1^3/144 - 3125\eta_1^4/48$$

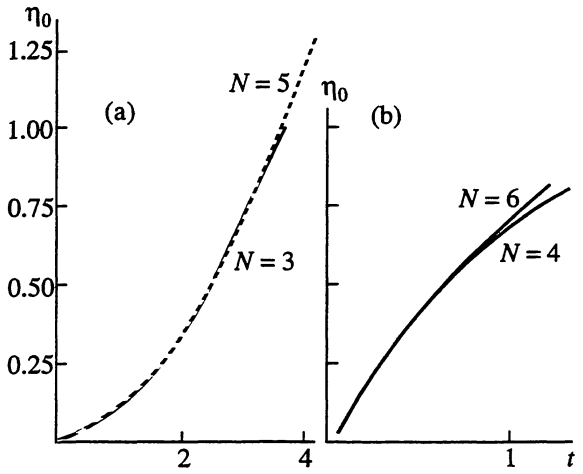

Fig. 2. Dependences $\eta_0(t)$. N is the number of harmonics taken into account. (a) Rayleigh–Taylor instability and (b) Richtmyer–Meshkov instability. The trajectories begin to diverge at time t_c.

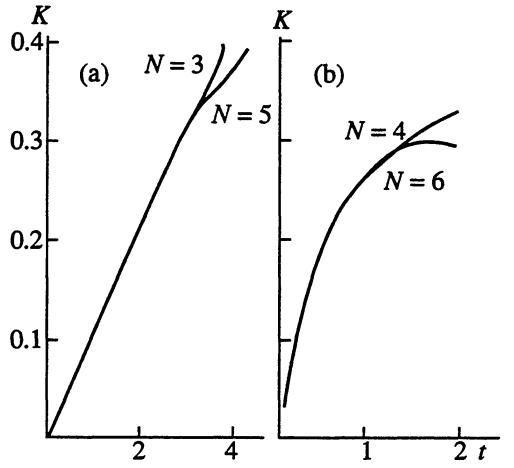

Fig. 3. Dependences $K(t)$. (a) Rayleigh–Taylor instability and (b) Richtmyer–Meshkov instability. The trajectories begin to diverge at time t_c.

$$
\begin{aligned}
&-125\eta_1^5/24 + 3125\eta_2/144 + 3125\eta_1\eta_2/24 \\
&+625\eta_1^2\eta_2/4 + 125\eta_1^3\eta_2/6 - 125\eta_2^2/4 \\
&-25\eta_1\eta_2^2/2 - 625\eta_3/24 - 125\eta_1\eta_3/2 \\
&-25\eta_1^2\eta_3/2 + 5\eta_2\eta_3 + 25\eta_4/2 + 5\eta_1\eta_4 - \eta_5.
\end{aligned}
$$

Matrix elements of the sixth order are omitted. The matrix $\hat{\Gamma}$ can be obtained from geometrical considerations, because this matrix depends on the changes of the boundary shape. In particular, for the flat boundary, we have $\eta_i = 0$ for $i = 1, 2, \ldots$, with the matrix $\hat{\Gamma}$ consisting of constant elements.

The main result of this study is that singularities on the boundary S_f were found. This is the result of the degeneration of the matrix $\hat{\Gamma}$ for infinite accelerations. The matrix determinant is

$$
\begin{aligned}
\det_1 &= -1/2 - \eta_1, \\
\det_2 &= -1/8 - 19\eta_1/24 - 3\eta_1^2/2 - \eta_1^3/2 - \eta_2/2, \\
\det_3 &= 1/48 + 389\eta_1/1440 + 661\eta_1^2/480 \\
&+ 10\eta_1^3/3 + 131\eta_1^4/36 + 3\eta_1^5/2 + \eta_1^6/6 \\
&+ \eta_2/4 + 3\eta_1\eta_2/2 + 2\eta_1^2\eta_2 + 2\eta_1^3\eta_2/3 \\
&- \eta_2^2/2 + \eta_3/4 + \eta_1\eta_3/2, \\
\det_4 &= 1/384 + 6893\eta_1/120960 \\
&+ 3927773\eta_1^2/7257600 + 17447\eta_1^3/6048 \\
&+ 1505057\eta_1^4/161280 + 16049\eta_1^5/864
\end{aligned}
$$

$$
\begin{aligned}
&+ 128089\eta_1^6/5760 + 545\eta_1^7/36 + 515\eta_1^8/96 \\
&+ 5\eta_1^9/6 + \eta_1^{10}/24 + 143\eta_2/2304 \qquad (12) \\
&+ 438091\eta_1\eta_2/483840 + 245\eta_1^2\eta_2/48 \\
&+ 3337\eta_1^3\eta_2/240 + 2795\eta_1^4\eta_2/144 + 427\eta_1^5\eta_2/32 \\
&+ 25\eta_1^6\eta_2/6 + 5\eta_1^7\eta_2/12 + \eta_2^2/5760 - 5\eta_1\eta_2^2/8 \\
&- 163\eta_1^2\eta_2^2/96 - 5\eta_1^3\eta_2^2/3 - 5\eta_1^4\eta_2^2/12 + 5\eta_2^3/4 \\
&+ 13\eta_1\eta_2^3/8 + 19\eta_3/192 + 5999\eta_1\eta_3/5760 \\
&+ 15\eta_1^2\eta_3/4 + 139\eta_1^3\eta_3/24 + 15\eta_1^4\eta_3/4 \\
&+ 19\eta_1^5\eta_3/24 - 61\eta_2\eta_3/96 - 5\eta_1\eta_2\eta_3/2 \\
&- 17\eta_1^2\eta_2\eta_3/8 - \eta_3^2/8 + 5\eta_4/48 + 61\eta_1\eta_4/96 \\
&+ 5\eta_1^2\eta_4/4 + 17\eta_1^3\eta_4/24 + \eta_2\eta_4/8,
\end{aligned}
$$

where the subscript on det designates the order of the system N. The expressions for $\det_5$ and $\det_6$ involve 126 and 395 terms, respectively, and, therefore, cannot be given in this paper.

The common trajectory with its origin in the vicinity of the hydrostatic equilibrium point cannot avoid the hypersurface det = 0 and necessarily reaches this hypersurface.

It should be noted that an assumption about the formation of singularities for $g = 0$ was recently proposed by Kuznetsov *et al.* [15], who observed the initial stage of motion of singularities to the surface S_f. Note, however, that these results do not allow one to conclude that this singularity will reach the surface S_f. First, this is

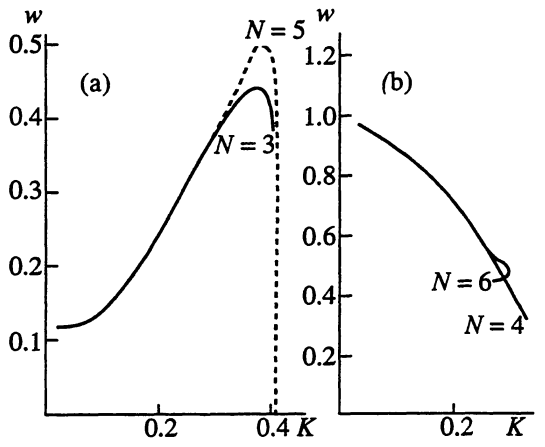

Fig. 4. Change of the bubble-top velocity $w(K)$. The curvature K is used as the independent variable instead of time. (a) Rayleigh–Taylor instability and (b) Richtmyer–Meshkov instability. The trajectories begin to diverge at time t_c.

due to the fact that the theory of weak nonlinearity is inapplicable near the singularity. The second argument, however, seems to be the most important. There are steady solutions with a singularity fixed at a distance on the order of unity from the surface S_f. Within the framework of the weakly nonlinear approximation, one cannot decide whether the evolution leads to the location of a singularity at a constant finite distance from the surface or whether the singularity coincides with the surface S_f.

The system of equations (11) was integrated using the predictor-corrector scheme with a variable integration step depending on the current error. The typical dependences on line of the shift of the top of the bubble $\eta_0(t)$ characterizing the dent effect are shown in Fig. 2. In Fig. 3, the inverse radius of curvature $K = 1/R$ is plotted as a function of time [where $R(t) = -1/(2\eta_1(t))$], which characterizes the distortion of S_f.

As is easily visible, the hydrostatic equilibrium is represented by the saddle point of (11), with incoming and outgoing separatrix. The eigenmodes are given by harmonics in (2). As follows from the direct linearization of (11), the eigenvalues are $\pm 1, \pm\sqrt{2}, \ldots, \pm\sqrt{N}$, where N is the order of the system. Initial perturbations of the principal mode with amplitudes of the velocity perturbation and/or location of the boundary that were not small in comparison with unity were used. Because of the hyperbolic nature of the hydrostatic equilibrium point, the trajectories are attracted to the outgoing separatrix even for arbitrary perturbation amplitudes. Therefore, the value $\eta_{0,c} = \eta_0(t_c)$, corresponding to the

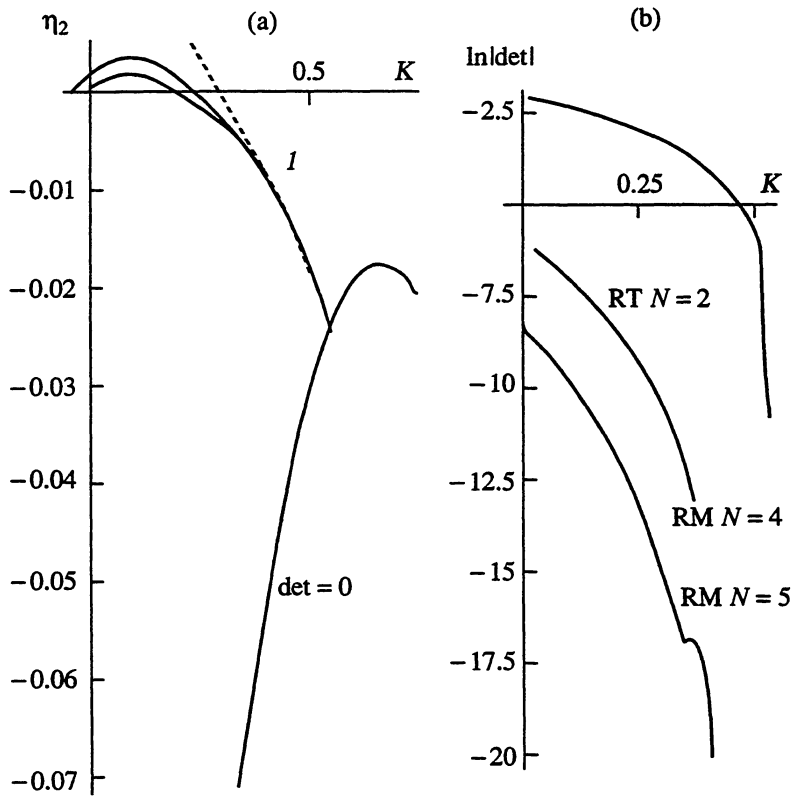

Fig. 5. Approaching the surface det = 0 for $N = 2$ and $g = 1$. (a) The change of *det* along the trajectory. The trajectories labeled by 1 correspond to different initial conditions. (b) During the motion, the system approaches the surface det = 0, and the quantity det falls by several orders of magnitude. Labels RT and RM correspond to the Rayleigh–Taylor instability and Richtmyer–Meshkov instability, respectively.

trajectory approaching the hypersurface D, where det = 0, depends weakly on initial conditions. For Rayleigh–Taylor instability, the corresponding time is obtained from the linear theory: $t_c = \ln(2\eta_{0,c}/(a_\eta + a_v))$, where a_η and a_v are the initial amplitudes measured along the corresponding direction cosines. This formula gives the logarithmic time delays for the appearance of a singularity because of the smallness of initial amplitudes. The quantity $\eta_{0,c}$ is discussed below.

As noted above concerning the initial conditions, we have $a_v = a_1(t = 0)$. Furthermore, because $\eta(x, t = 0) = \eta_0(0) + \eta_1(0)x^2 + \eta_2(0)x^4 + \ldots$ [see formula (3)] and, on the other hand, $\eta(x, t = 0) = a_\eta \cos x$, then $\eta_n(t = 0) = (-1)^n/(2n)!$, for $n = 0, 1, 2, \ldots$.

These variables are shown in Figs. 2 and 3 as a function of time. Because these quantities depend on initial conditions,[1] it is more convenient to consider the change of geometrical characteristics instead of time, because they are less sensitive to initial conditions. For this reason, in the following figures, the motion along the trajectory is parameterized by the curvature K.

The change of the bubble-top velocity w along the trajectory is shown in Fig. 4. From calculations, we found that, upon the appearance of singularity, the parameters are

$$\eta_{0,c} \approx 0.75\ (g = 1), \quad \eta_{0,c} \approx 0.55\ (g = 0),$$
$$K_c \approx 0.28\ (g = 1), \quad K_c \approx 0.25\ (g = 0),$$
$$w_c \approx 0.36\ (g = 1), \quad w_c \approx 0.59\ (g = 0).$$

These parameters are called critical. The trajectory does not intersect the surface det = 0 only for $N = 1$. Otherwise, the parameters are virtually the same for any N. Note that the case with $g = 1$ and $N = 1$ was considered by Layzer [16].

The trajectory of the system with $g = 2$ and $N = 2$ is shown in Fig. 5a. For $N = 2$, there are only two geometrical characteristics: $\eta_1 = -K/2$ and η_2. Therefore, the trajectory in the geometrical space (η_1, η_2), as well as the surface det = 0, can be represented in the plane diagram. As is shown, the system approaches the surface det = 0, and trajectories intersect the surface. The trajectories are labeled by the index 1 and correspond to different initial conditions. Note also that trajectories tighten with time.

The decline of det with time is shown in Fig. 5b; as is evident, det decreases for all trajectories. The drop of det by several orders of magnitude implies that the system closely approaches the surface det = 0.

This work was financially supported by the Russian Foundation for Fundamental Research (project no. 93-02-3630).

[1] For example, the Rayleigh–Taylor instability with large time delays around the hydrostatical equilibrium and small amplitudes of initial perturbations.

REFERENCES

1. Gull, S.F., *Mon. Not. R. Astron. Soc.*, 1975, vol. 171, p. 263.
2. McKee, C.F., *Astrophys. J.*, 1974, vol. 188, p. 335.
3. Imshennik, V.S. and Nadezhin, D.K., *Itogi Nauki i Tekhniki, Ser.: Astron.*, Moscow: VINITI, 1982, vol. 21, p. 63.
4. Grebenev, S.A. and Syunyaev, R.A., *Pis'ma Astron. Zh.*, 1987, vol. 13, p. 945.
5. Arnett, D., Fryxell, B., and Muller, E., *Astrophys. J.*, 1989, vol. 341, p. L63.
6. Ebisuzaki, T., Shigeyama, T., and Nomoto, K., *Astrophys. J.*, 1989, vol. 344, p. L65.
7. Den, M., Yoshida, T., and Yamada, Y., *KEK Rep.*, 1990, vol. 89, p. 173.
8. Hachisu, I., Matsuda, T., Nomoto, K., and Shigeyama, T., *KEK Rep.*, 1990, vol. 89, p. 185.
9. Kahn, F.D., *Planetary Nebulae, IAU Symp. no. 103*, Flower, D.R., Ed., Dordrecht: Reidel, 1983, p. 305.
10. Igumenshchev, I.V., personal communication, 1989.
11. Dibai, E.A., *Astron. Zh.*, 1958, vol. 35, p. 469.
12. Arons, J. and Lea, S.M., *Astrophys. J.*, 1976, vol. 207, p. 914.
13. Elsner, R.F., *PhD Dissertation*, Champaign–Urbana: Univ. of Illinois, 1976.
14. Karpinskii, V.N., Some Problems of Solar Hydrodynamics, *Tr. Symp. po Aktual'nym Problemam Astrofiziki i Geofizicheskoi Gidrodinamiki* (Proc. Symp. on Modern Problems in Astrophysics and Geophysical Hydrodynamics), Svetlogorsk, 1994 (in press).
15. Kuznetsov, E.A., Spektor, M.D., and Zakharov, V.E., *Phys. Lett. A*, 1994 (in press).
16. Layzer, D., *Astrophys. J.*, 1955, vol. 122, p. 1.